Effects of Lung Expansion on Global and Regional Pulmonary Blood Volume in a Sheep Model of Acute Lung Injury

Mingyang Zang, Congli Zeng, David Lagier, Nan Leng, Kira Grogg, Gabriel Motta-Ribeiro, Andrew Laine, Tilo Winkler, Marcos Vidal Melo

ANESTHESIOLOGY®

Effects of Lung Expansion on Global and Regional Pulmonary Blood Volume in a Sheep Model of Acute Lung Injury

Mingyang Zang, M.S., Congli Zeng, M.D., Ph.D., David Lagier, M.D., Ph.D., Nan Leng, M.S.E.D., Kira Grogg, Ph.D., Gabriel Motta-Ribeiro, Ph.D., Andrew F. Laine, Ph.D., Tilo Winkler, Ph.D., Marcos F. Vidal Melo, M.D., Ph.D.

ANESTHESIOLOGY 2025; 142:1071–84

EDITOR'S PERSPECTIVE

What We Already Know about This Topic

- Pulmonary capillary blood volume plays a major role in gas transport efficiency within the lungs, because it is a key factor in determining pulmonary diffusing capacity
- The question of how lung expansion influences pulmonary capillary blood volume in the injured lung remains incompletely understood

What This Article Tells Us That Is New

- In a sheep model of endotoxemic lung injury with low-volume mechanical ventilation, dynamic assessment of whole-lung and regional blood and gas volume distributions with positron emission tomography/computed tomography revealed marked heterogeneity in the spatial distribution of pulmonary capillary blood volume with strong dependence on lung expansion and vertical variation
- Tissue-normalized blood volumes in nondependent lung regions were substantially lower, indicating susceptibility to capillary closure
- Recruitment of pulmonary vascular blood volume with gas volume was nonlinear, and intermediate positive end expiratory pressure levels of 12 cm H_2O resulted in the most homogenous distribution of tissue-normalized blood volume in this experimental model

ABSTRACT

Background: Pulmonary capillary blood volume is a major determinant of lung gas transport efficiency and also potentially related to ventilator-induced lung injury. However, knowledge on how lung expansion influences pulmonary blood volume in injured lungs is scant. The hypothesis was that lung expansion produced by positive end-expiratory pressure (PEEP) modulates the global and regional spatial distribution of pulmonary blood volume.

Methods: In a lung injury model exposed to distinct lung expansion within clinical range (PEEP of 5 to 20 cm H_2O), this study aimed to determine whole-lung and regional blood volume, their dynamic changes, and association with gas volume changes. Seven healthy sheep were subjected to 3 h of low-lung volume mechanical ventilation at a PEEP of 0 cm H_2O and systemic endotoxemia. PEEP values of 5 (low), 20 (high), and 12 (intermediate) cm H_2O were applied to produce distinct lung expansion. Respiratory-gated positron emission tomography with ^{11}C-labeled carbon monoxide and four-dimensional computed tomography were obtained to quantify blood volume and aeration.

Results: Transpulmonary pressures were lowest at a PEEP of 12 cm H_2O. Changes in whole-lung blood volume correlated with gas volume changes between PEEP of 5 and 12 cm H_2O at end expiration ($P < 0.001$) and end inspiration ($P < 0.001$) but not between 12 and 20 cm H_2O. Tissue-normalized blood volume ($V_{B_{tissue}}$) was heterogeneously distributed, with mean values in nondependent regions ($V_{B_{tissue}} = 0.116 \pm 0.055$) approximately seven times smaller than those in mid-dependent regions ($V_{B_{tissue}} = 0.832 \pm 0.132$). A positive end-expiratory pressure of 12 cm H_2O resulted in the most homogeneous $V_{B_{tissue}}$ distribution, with the largest means in mid-dependent regions and inspiratory 10th percentile, a measure of lowest values, throughout the lung. $V_{B_{tissue}}$ increased with inspiration at PEEP of 5 and 12 cm H_2O but decreased with a PEEP of 20 cm H_2O in mid-nondependent regions.

Conclusions: During low-volume mechanical ventilation and systemic endotoxemia, lung blood volume is markedly heterogeneously distributed, and modulated by PEEP. Nondependent regions are susceptible to low blood volume and capillary closure. Recruitment of pulmonary vascular blood volume with gas volume is nonlinear, limited at an intermediate PEEP, indicating its advantage to spatial distribution of blood volume.

(ANESTHESIOLOGY 2025; 142:1071–84)

Pulmonary capillary blood volume (V_C) is a major determinant of gas transport efficiency in the lungs because it is a primary component of pulmonary diffusing capacity.[1,2] Recent studies also suggest that reduction in V_C during mechanical ventilation could promote ventilator-induced

Supplemental Digital Content is available for this article. Direct URL citations appear in the printed text and are available in both the HTML and PDF versions of this article. Links to the digital files are provided in the HTML text of this article on the Journal's Web site (www.anesthesiology.org). M.Z. and C.Z. contributed equally to this article.

Submitted for publication June 12, 2024. Accepted for publication February 3, 2025. Published online first on February 12, 2025.

Mingyang Zang, M.S.: Department of Biomedical Engineering, Columbia University, New York, New York.

Congli Zeng, M.D., Ph.D.: Department of Anesthesiology, Vagelos College of Physicians and Surgeons, Columbia University, New York, New York.

David Lagier, M.D., Ph.D.: Experimental Interventional Imaging Laboratory, European Center for Research in Medical Imaging, Aix Marseille University, Marseille, France.

Nan Leng, M.S.E.D.: Department of Anesthesiology, Vagelos College of Physicians and Surgeons, Columbia University, New York, New York.

Kira Grogg, Ph.D.: Department of Radiology, Massachusetts General Hospital, Boston, Massachusetts.

 ANESTHESIOLOGY 2025; 142:1071–84. DOI: 10.1097/ALN.0000000000005412

<zdoi;10.1097/ALN.0000000000005412>

lung injury.[3,4] Indeed, tidal interruption of blood flow in pulmonary capillaries during large tidal volume mechanical ventilation produced microvascular injury in small animal models of ventilator-induced lung injury.[3,4] Importantly, areas of very low or no perfusion have been described in injured large animal lungs with ventilatory settings consistent with clinical practice,[5] suggesting susceptibility to microvascular/endothelial injury in lungs anatomically and functionally comparable to human lungs. Notably, in mechanically ventilated surgical patients, reduction in V_C has been associated to alveolar-capillary damage.[6]

Lung expansion produced by positive pressure mechanical ventilation could importantly influence V_C in opposing directions. V_C has been reported to be reduced by mechanical ventilation in individuals with normal lungs as compared to spontaneous ventilation[7,8] and further decreased by lung expansion with positive end-expiratory pressure (PEEP).[7,9] This has been explained by increased intrathoracic and airway pressures reducing venous return and increasing alveolar pressures above pulmonary artery pressures producing West zone I conditions[10] with continuous or cyclic capillary closure.[5,11,12] In contrast, alveolar recruitment produced by PEEP could *increase* V_C as a result of capillary recruitment and/or vascular expansion.[8] Indeed, in a subset of patients with adult respiratory distress syndrome, application of PEEPs of 15 *versus* 5 cm H_2O resulted in increased V_C, indicating functional pulmonary vascular recruitment.[8] However, there is currently little knowledge on how lung expansion influences the magnitude and spatial distribution of pulmonary blood volume in injured mechanically ventilated lungs and consequently modulates such potential lung injury mechanisms.

Previous positron emission tomography (PET) studies have described a ventral–dorsal positive gradient in pulmonary blood volume[13] and perfusion[14] in spontaneously breathing humans and blood volume[15,16] and perfusion[5,17] in mechanically ventilated lung injured sheep. Recent dual-energy computed tomography (CT) data indicated a tidal inspiratory redistribution of blood volume toward poorly ventilated lung in surfactant-depleted pigs with significant atelectasis.[18] These studies were limited by low-resolution, single-slice, or large-region-of-interest analyses, and not systematically addressing lung expansion effects.[13,18–20] In the current study, we use techniques of respiratory-gated PET and high-resolution CT to quantify pulmonary blood volume and aeration.

Gabriel Motta-Ribeiro, Ph.D.: Biomedical Engineering Program, Alberto Luiz Coimbra Institute for Graduate Studies and Research in Engineering, Universidade Federal do Rio de Janeiro, Rio de Janeiro, Brazil.

Andrew F. Laine, Ph.D.: Department of Biomedical Engineering, Columbia University, New York, New York.

Tilo Winkler, Ph.D.: Department of Anesthesia, Critical Care and Pain Medicine, Massachusetts General Hospital, Harvard Medical School, Boston, Massachusetts.

Marcos F. Vidal Melo, M.D., Ph.D.: Department of Anesthesiology, Vagelos College of Physicians and Surgeons, Columbia University, New York, New York.

We hypothesize that lung expansion modulates global and regional distribution of pulmonary blood volume and that global pulmonary blood volume increases with gas volume recruitment, with a stronger relationship from derecruited to recruited states, *i.e.*, low to moderate levels of lung expansion, but less so at recruited states, *i.e.*, from moderate to high levels. We further theorize that spatial redistribution of blood volume in these conditions produces very low values in nondependent regions, consistent with susceptibility to lung injury. To test these hypotheses, we assessed dynamic whole-lung and regional blood and gas volume distributions with PET/CT in a large animal model of acute lung injury with aeration heterogeneity comparable to that of humans and distinct lung expansion produced with PEEP at a broad range consistent with clinical values.

Materials and Methods

All animal procedures were approved by the Subcommittee on Research Animal Care and the Institutional Animal Care and Use Committee of the Massachusetts General Hospital (approval no. 2018N000165; study title: PET/CT-guided personalized mechanical ventilation to minimize ventilator-induced lung injury; approval date: November 26, 2018) and in accordance with the Guide for the Care and Use of Laboratory Animals published by the National Institutes of Health (publication no. 86-23, revised 1996)[21] and in adherence to the Animal Research: Reporting of *in vivo* Experiments (ARRIVE) guidelines.[22] Full details on the Materials and Methods are found in the supplemental digital content (https://links.lww.com/ALN/D889).

Experimental Protocol

Seven healthy sheep of both sexes (*Ovis aries*, 22.2 ± 2.4 kg, male/female 3/4) were premedicated and intubated. Anesthesia was maintained with a continuous infusion of propofol ($5\ mg \cdot kg^{-1} \cdot h^{-1}$) and xylazine ($50\ \mu g \cdot kg^{-1} \cdot h^{-1}$). Paralysis was established with a rocuronium bolus at induction (0.5 mg/kg) and subsequent continuous infusion ($0.5\ mg \cdot kg^{-1} \cdot h^{-1}$). Acute lung injury with lung derecruitment was induced by 3 h of low-volume mechanical ventilation and systemic endotoxemia. Mechanical ventilation settings were: volume-control mode; tidal volume = 8 ml/kg; PEEP = 0 cm H_2O; F_{IO_2} = 1; I:E ratio = 1:2; and RR = 25 breaths/min, adjusted to maintain the arterial carbon dioxide partial pressure between 32 and 45 mmHg. Systemic endotoxemia was induced by continuous systemic injection of lipopolysaccharide (10 ng/kg/min), which was started at beginning of injurious mechanical ventilation. After 3 h, the animals were transferred to the PET/CT imaging suite and received three different levels of lung expansion produced by PEEP applied in the order of 5 (low), 20 (high), and 12 cm H_2O (intermediate). This order was used to provide a well established low lung expansion

state (PEEP = 5 cm H_2O),[23] a high expansion state within clinical values (PEEP = 20 cm H_2O),[24] and an intermediate expansion state at PEEP = 12 cm H_2O, a level consistent with average lower transpulmonary and respiratory system driving pressures and highest compliance in animals[25] and patients[26–28] and associated with biomechanical benefits when established from a recruited state.[23] After a period of stabilization, cardiopulmonary variables were collected, and dynamic four-dimension PET/CT imaging scans[29,30] were performed at each PEEP setting.

Image Acquisition

[^{11}C]Carbon monoxide binds to hemoglobin with an affinity 200 times that of oxygen to form ^{11}C-labeled carboxyhemoglobin ([^{11}C]CO-Hb).[31] [^{11}C]CO-Hb was used to estimate total hemoglobin concentration, which is positively related to blood volume. [^{11}C]CO gas with measured doses at injection time ranges between 20 and 54 mCi (33.10 ± 15.74, n = 7) was produced immediately preceding the experiment, delivered into a rebreathing circuit connected with the animal's mechanical ventilator and allowed to equilibrate for at least 1 min. After this equilibration, PET/CT imaging was started using respiratory-gated positron emission tomography (GE Discovery MI PET/CT[32]; GE Healthcare, USA). The respiratory signal was added to the list mode data using input to the scanner from the ventilator system. A single bed position covering 25 cm and encompassing the whole lung was acquired for at least 10 min. PET images were divided into 15 time epochs and reconstructed using an ordered-subset expectation maximum algorithm with resolution and time-of-flight corrections, resulting in an image matrix of 256 × 256 × 89 × 15 with a thickness of 2.8 mm and in-plane resolution of 1.953 mm. The inspiratory and expiratory images were built from average images obtained during stable end-inspiratory and end-expiratory periods within those 15 time epochs. Transpulmonary and respiratory system driving pressures, as well as end-tidal pressure of carbon dioxide, systemic and pulmonary artery pressures were monitored at each PEEP level, and images were only acquired once those measurements were stable.

Segmentation of global lung volumes was performed in two steps: (1) a deep-learning algorithm used to segment the whole lung with exclusion of main bronchi and vessels[33] and (2) a semi-automatic algorithm to exclude lung regions affected by partial volume effect and misalignment of PET and computed tomography images.[34]

Imaging Analysis

CT and lung masks were downsampled to the PET resolution. Two conditions' end expiration and end inspiration at each PEEP with their corresponding CT and PET frames were investigated. Regional lung analysis was conducted in a nondependent to dependent (vertical) direction, with the total lung region divided into 10 regions of interest (ROIs) with equal height along the vertical axis.

Aeration. Lung aeration was computed from Hounsfield units (HUs) as voxel gas fraction (F_{gas}) = HU/−1,000 with air = −1,000 HU (F_{gas} = 1) and tissue = 0 HU (F_{gas} = 0).[30] The sizes of hyperaerated ($F_{gas} \geq 0.9$), normally aerated ($0.5 \leq F_{gas} < 0.9$), poorly aerated ($0.1 \leq F_{gas} < 0.5$), and nonaerated ($F_{gas} < 0.1$) regions were expressed as percentages of the total lung mass, defined as $\sum_{\text{voxels in ROI}} \text{voxel volume} \times (1 - F_{gas})$. Voxel volume = 0.011 ml.

Blood Volume. [^{11}C]CO gas was delivered with the use of a closed rebreathing system. Blood fraction (F_{blood}) was computed by normalizing the voxel-level raw [^{11}C]CO activity to the mean [^{11}C]CO activity in the descending aorta (average volume V_{aorta} =2.06 ± 0.71 cm^3, n = 7). Blood volume (V_B) was calculated as F_{blood} × voxel volume. The ROI in the aorta was manually segmented with a customized toolbox in MATLAB. Blood volume (V_B) was then calculated by multiplying F_{blood} with voxel volume at PET resolution.

$$F_{blood} = \frac{\text{voxel} - \text{level}[^{11}\text{C}]\ \text{CO activity}}{\frac{\sum_{\Omega}[^{11}\text{C}]\text{CO activity}}{|\ \Omega\ |}} \quad (1)$$

$$V_B = F_{blood} \times \text{voxel volume} \quad (2)$$

where Ω indicates the voxels in the descending aorta.

Tissue-normalized Blood Volume. Because lung inflation differs in different regions and tidally, V_B was normalized to tissue volume. For this, CT was used to compute the voxel density fraction ($1 - F_{gas}$), and lung tissue volume was computed as the amount of tissue excluding blood volume (V_{tissue} = [1 − F_{gas} − F_{blood}] × voxel volume). Tissue-normalized blood volume ($V_{B_{tissue}}$) was calculated as $V_{B_{tissue}} = V_B/V_{tissue}$.

Gas-normalized Blood Volume. The ratio of regional V_B to gas volume (V_G), a usual whole-lung normalization,[35] was applied at the local level as $V_{Bgas} = V_B/V_G$, where $V_G = F_{gas}$ × voxel volume.

Spatial Heterogeneity. The spatial heterogeneity of F_{gas} and $V_{B_{tissue}}$ were assessed by the coefficient of variation (COV) in end-expiratory and end-inspiratory images as done previously.[36] COV = σ/μ, where σ = SD, and μ = mean of voxel-level values.

Study Outcomes

Our primary outcome was the tissue-normalized pulmonary blood volume. The secondary outcome variables were the whole-lung and regional pulmonary blood volume and lung aeration. We studied the relationship between those

blood volume changes and the corresponding whole-lung and regional gas volume changes between PEEP levels, as well as between end expiration and end inspiration.

Statistical Analyses

Because no published data on tissue normalized blood volume are available, we used measurements of regional blood flow,[37] known to be related to blood volume,[15,19] to compute sample size. In that previous study, regional blood flow fraction in dependent lung regions between levels of lung expansion similar to those studied in the current study produced a change from 0.66 ± 0.10 to 0.52 ± 0.08, yielding an estimated sample size of at least six animals for an α error = 0.05, power = 80%, and *t* test with matched pairs; we studied seven animals.

The data are presented as means ± SD. Physiologic data for each of the three levels of lung expansion (PEEPs of 5, 12, and 20 cm H_2O) were compared with one-way mixed-effects models. A two-way repeated measures ANOVA was used to study the effect of lung expansion levels on total lung gas volumes and total lung blood volumes with an interaction term between breathing phase and PEEP. Two-way mixed-effects models were used to study the effect of lung expansion levels and regional distribution (10 vertical ROIs) on the end-inspiratory to end-expiratory changes in $V_{B_{tissue}}$ and gas fractions, with an interaction term between ROIs and PEEP. The effect of lung expansion levels, breathing phase (end expiration and end inspiration), and regional distribution (10 vertical ROIs) for the measured regional gas fractions, blood volume per voxel, tissue-normalized blood volume and its 10th percentile, and gas-normalized blood volume were quantified with repeated measures ANOVA with interaction terms for each combination of ROI, PEEP, and breathing phase. We quantified the relationship between changes in whole-lung blood volume (*y*-axis) and gas-volume (*x*-axis) for each pair of lung expansion levels (PEEPs of 5 and 20, 5 and 12, or 20 and 12 cm H_2O) at end expiration and end inspiration, as well as between end expiration and end inspiration for each of the three lung expansion levels using mixed-effects regressions. Differences between the slopes of all PEEP levels were compared *via* interaction terms. We used the Greenhouse–Geisser method to correct nonsphericity in the mixed-effects and ANOVA models. One animal had missing data and was excluded from all ANOVA and regression models. The data were analyzed using GraphPad Prism (version 10.2.0; GraphPad Software, USA) and R (version 4.3.2; R Core Team, Austria).[38] Tests were two-tailed, and significance was considered at $P < 0.05$.

Results

Global Cardiopulmonary Function

At baseline, respiratory and cardiovascular variables were normal and consistent with atelectasis from general anesthesia and mechanical ventilation (supplemental table S1). After 3 h of low–lung volume mechanical ventilation and systemic endotoxemia, mean P_{AO_2}/F_{IO_2} was consistent with moderate acute respiratory distress syndrome (ARDS) at a PEEP of 5 cm H_2O during imaging (table 1). Peak ($P < 0.001$) and plateau ($P < 0.001$) pressures were significantly higher with larger PEEP (table 1). A PEEP of 12 cm H_2O resulted in the lowest driving ($P < 0.001$) and transpulmonary ($P < 0.001$) pressures with the corresponding highest respiratory system ($P = 0.004$) and lung ($P = 0.007$) compliance (table 1). A PEEP of 20 cm H_2O reduced cardiac output ($P = 0.008$) and increased mean pulmonary artery pressure ($P < 0.001$) and pulmonary capillary wedge pressure ($P = 0.001$; table 1).

Lung Aeration

Lung aeration was heterogeneously distributed in these acutely injured lungs, which was particularly evident at a PEEP of 5 cm H_2O (fig. 1A). PEEP produced an increase in lung aeration ($P = 0.007$; fig. 2A), accompanied by decreased aeration heterogeneity (*i.e.*, coefficient of variation) at both end expiration ($P < 0.001$) and end inspiration ($P < 0.001$; table 1). Normally aerated lung mass was predominantly present at all PEEPs, followed by poorly aerated and nonaerated lung mass as well as negligible hyperinflation (fig. 2, C and D). Lung aeration in each vertical ROI was consistently increased with PEEP (ROI × PEEP: $P < 0.001$; fig. 2E).

Lung Blood Volume

Whole-lung blood volume (V_B; fig. 2B) was not only different at different PEEPs ($P = 0.046$) and respiratory breathing phases ($P = 0.013$) but also showed different values at the breathing phases depending on PEEP (phase × PEEP: $P = 0.025$). Whole-lung V_B increased from PEEPs of 5 to 20 cm H_2O but did not change significantly from PEEPs of 20 to 12 cm H_2O at both end-expiration and end-inspiration. This contrasted with the continuous increase of whole-lung gas volume (V_G) with PEEP (fig. 2A). As expected, V_B showed a strong gravitational dependence ($P < 0.001$; fig. 2F), with the largest V_B localized dorsally both at end expiration and end inspiration. At each ROI, V_B gradually decreased as PEEP increased, with the lowest V_B observed at PEEP = 20 cm H_2O (ROI × PEEP: $P < 0.001$; fig. 2F).

Whole-lung Blood Volume *versus* Gas Volume Changes

Whole-lung V_B increases from PEEP = 5 to 20 cm H_2O directly related to whole-lung V_G increases at end expiration ($P < 0.001$; fig. 3A) and end inspiration ($P = 0.037$; fig. 3B). Such a relationship was also observed from PEEPs of 5 to 12 cm H_2O at end expiration ($P < 0.001$) and at end inspiration ($P < 0.001$; fig. 3, A and B). Of note, the regression line for PEEPs of 5 to 12 cm H_2O showed a

Table 1. Respiratory and Cardiovascular Variables as Well as Whole-lung Aeration and Tissue-normalized Blood Volume at Three PEEP Levels

Variable	PEEP 5 cm H_2O	PEEP 20 cm H_2O	PEEP 12 cm H_2O	*P* Value
Respiratory variables				
V_T, ml/kg	8.4 ± 0.3	8.9 ± 0.3	8.6 ± 0.8	0.222
RR, min^{-1}	20 ± 0	20 ± 0	20 ± 0	
P_{peak}, cm H_2O	20.8 ± 2.1	36.7 ± 2.6	23.1 ± 3.5	< 0.001
$P_{plateau}$, cm H_2O	19.3 ± 2.1	35.5 ± 2.3	21.6 ± 3.4	< 0.001
DP, cm H_2O	14.0 ± 1.8	16.4 ± 1.8	9.8 ± 2.7	< 0.001
P_{TP}, cm H_2O	11.1 ± 0.9	12.6 ± 1.6	6.8 ± 2.2	< 0.001
C_{RS}, cm $H_2O \cdot l^{-1} \cdot s^{-1}$	13.1 ± 2.5	12.0 ± 1.2	20.0 ± 4.2	0.004
C_L, ml/cm H_2O	16.5 ± 2.1	15.7 ± 2.1	29.4 ± 8.6	0.007
PaO_2, mmHg	119 ± 75	145 ± 156	144 ± 111	0.546
FIO_2, %	81 ± 21	83 ± 22	87 ± 22	0.261
PaO_2/FIO_2	156 ± 99	185 ± 146	173 ± 157	0.579
Cardiovascular variables				
Heart rate, beats/min	105 ± 7	115 ± 23	129 ± 41	0.272
CO, l/min	4.3 ± 1.2	2.6 ± 0.8	3.6 ± 1.0	0.008
PCWP, mmHg	11.2 ± 5.4	17.6 ± 5.7	16.4 ± 5.0	0.001
PAP_{syst}, mmHg	26 ± 5	38 ± 5	36 ± 11	0.009
PAP_{dia}, mmHg	17 ± 5	26 ± 6	24 ± 9	< 0.001
MPAP, mmHg	22 ± 5	31 ± 6	29 ± 9	< 0.001
MAP, mmHg	90 ± 15	75 ± 15	91 ± 14	0.098
PVR, dyn/s/cm	231 ± 37	405 ± 150	352 ± 136	0.086
Aeration (F_{gas})				
Mean (EE)	0.61 ± 0.05	0.73 ± 0.05	0.69 ± 0.07	< 0.001
COV (EE)	0.44 ± 0.11	0.28 ± 0.10	0.33 ± 0.12	< 0.001
Mean (EI)	0.66 ± 0.04	0.76 ± 0.05	0.72 ± 0.06	< 0.001
COV (EI)	0.40 ± 0.11	0.26 ± 0.10	0.31 ± 0.11	< 0.001
Tissue-normalized blood volume ($V_{B_{tissue}}$)				
Mean (EE)	0.65 ± 0.12	0.63 ± 0.08	0.64 ± 0.12	0.841
COV (EE)	0.69 ± 0.09	0.66 ± 0.07	0.65 ± 0.09	0.455
Mean (EI)	0.70 ± 0.14	0.61 ± 0.11	0.70 ± 0.12	0.314
COV (EI)	0.76 ± 0.09	0.69 ± 0.08	0.64 ± 0.08	0.046

The variables are presented as means ± SD. The associated *P* values refer to the test of the null hypothesis that the means of the tested variable in each group are equal and derived from a one-way mixed-effects models.

C_L, lung compliance; CO, cardiac output; COV, coefficient of variation; C_{RS}, respiratory system compliance; DP, driving pressure; EE, end expiration; EI, end inspiration; F_{gas}, gas fraction; FIO_2, inspired oxygen fraction; MAP, mean arterial pressure; MPAP, mean pulmonary arterial pressure; P_{peak}, peak airway pressure; $P_{plateau}$, plateau airway pressure; P_{TP}, transpulmonary pressure; PaO_2, ratio of arterial partial pressure of oxygen; PaO_2/FIO_2, ratio of PaO_2 to FIO_2; PAP_{dia}, diastolic pulmonary arterial pressure; PAP_{syst}, systolic pulmonary arterial pressure; PCWP, pulmonary capillary wedge pressure; PEEP, positive end-expiratory pressure; PVR, pulmonary vascular resistance; RR, respiratory rate; V_T, tidal volume.

larger slope than that for PEEPs of 5 to 20 cm H_2O at end inspiration ($P = 0.043$), implying a larger whole-lung V_B change with V_G for PEEPs of 5 to 12 than for PEEPS of 5 to 20 cm H_2O. Whole-lung V_B from end expiration to end inspiration increased with V_G at a PEEP of 12 cm H_2O ($P = 0.003$) but decreased with V_G at a PEEP of 20 cm H_2O ($P = 0.021$; fig. 3C). In contrast, no significant relationship was found from changes between PEEPs of 12 and 20 cm H_2O at both breathing phases (fig. 3, A and B) or from end expiration to end inspiration at a PEEP of 5 cm H_2O (fig. 3C).

Blood Volume Normalized to Tissue Volume

Whole-lung Level. To account for the change in lung expansion on the assessment of blood volume, we computed voxel-wise V_B normalized to tissue volume ($V_{B_{tissue}}$; fig. 1, B and C). Despite the comparable mean whole-lung $V_{B_{tissue}}$ at all PEEPs, the end-inspiratory heterogeneity of $V_{B_{tissue}}$ (*i.e.*, coefficient of variation) was lower (most homogeneous spatial distribution) at a PEEP of 12 cm H_2O than at PEEPs of 5 or 20 cm H_2O ($P = 0.046$; table 1).

Regional Distribution. Regional distributions of $V_{B_{tissue}}$ revealed a significant gravitational dependence, *i.e.*, a ROI effect ($P < 0.001$), as well as effects of the breathing phase cycle ($P = 0.040$; fig. 4A). Regional $V_{B_{tissue}}$ was observed with high levels in the middle to dependent lung areas, particularly with a PEEP 12 cm H_2O at both end expiration ($V_{B_{tissue}} = 0.744 \pm 0.141$) and end inspiration ($V_{B_{tissue}} = 0.832 \pm 0.132$; fig. 4A). In contrast, the lowest $V_{B_{tissue}}$ was predominantly found in nondependent lungs with a PEEP of 20 cm H_2O (fig. 4A).

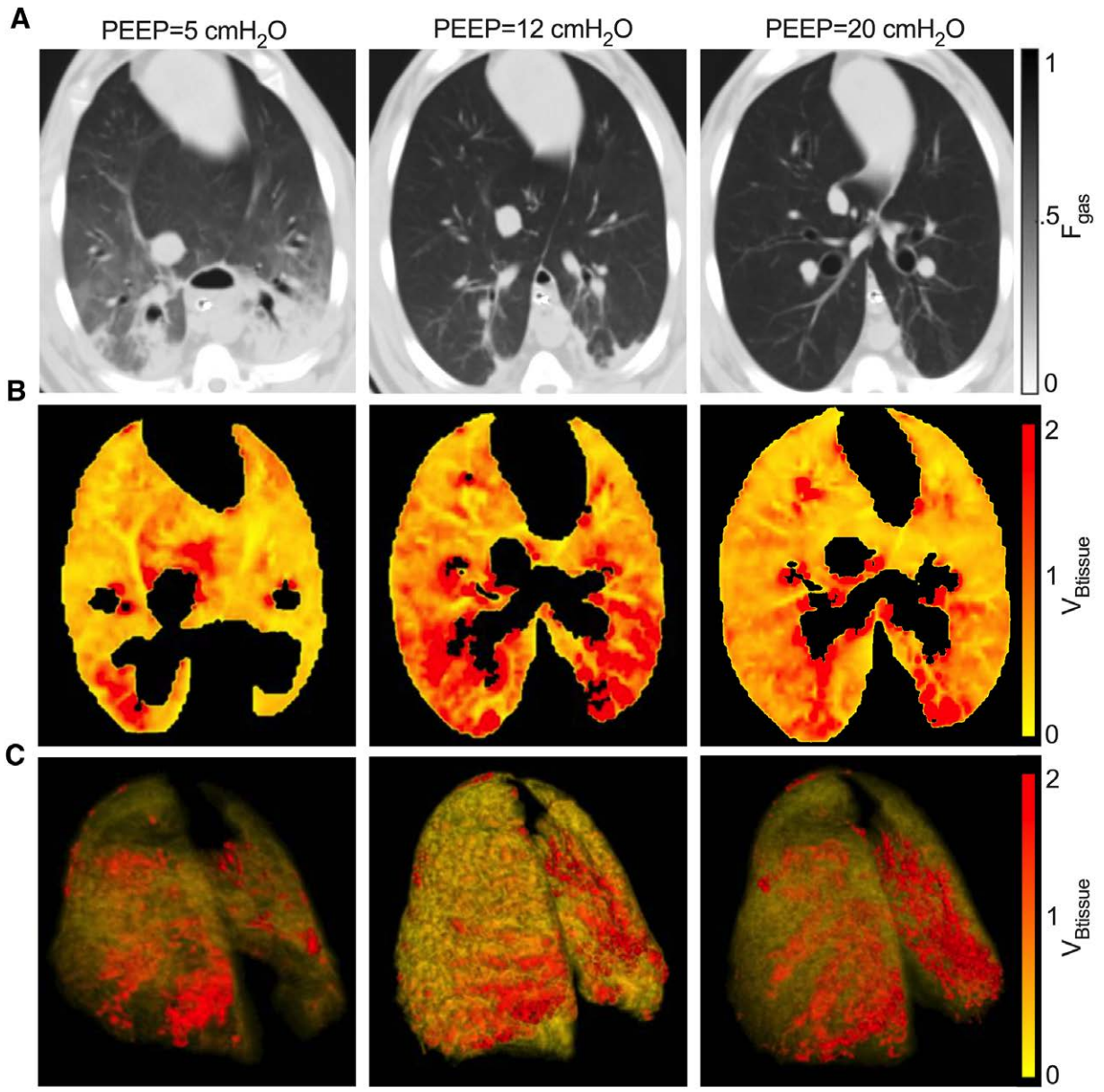

Fig. 1. (*A*) Computed tomography (CT) images with aeration ranges with positive end-expiratory pressures (PEEPs) of 5, 12, and 20 cm H_2O at end expiration. Lung gas fraction (F_{gas}) increased (darker parenchyma) with PEEPs. (*B*) Tissue-normalized blood volume ($V_{B_{tissue}}$) computed at the voxel level with PEEPs of 5, 12, and 20 cm H_2O at end inspiration. Axial slices at approximately two-thirds of the cephalocaudal axis showing voxel level $V_{B_{tissue}}$. *Yellow*, lower $V_{B_{tissue}}$; *red*, higher $V_{B_{tissue}}$. (*C*) Three-dimensional rendering of $V_{B_{tissue}}$ with PEEPs of 5, 12, and 20 cm H_2O at end inspiration in the same representative animal. The values are color coded from low (*yellow*) to high (*red*). The values at lowest value ($V_{B_{tissue}}$ =0) of the scale were 100% transparent with a gradual increase in opacity to the highest value ($V_{B_{tissue}}$ = 2).

The 10th percentile of $V_{B_{tissue}}$, a measure of the lowest range of $V_{B_{tissue}}$, also presented gravitational dependent distributions ($P < 0.001$; fig. 4B), with the lowest 10th percentile of $V_{B_{tissue}}$ in the most nondependent region at all PEEPs (0.116 ± 0.055). A PEEP of 12 cm H_2O yielded a higher 10th percentile of $V_{B_{tissue}}$ throughout the whole-lung at end inspiration and in dependent regions at end expiration (fig. 4B). The 10th percentile of $V_{B_{tissue}}$ was similar at all PEEPs in nondependent regions at end expiration (fig. 4B).

Intratidal changes in $V_{B_{tissue}}$ presented gravitational dependence with marked changes in middle to dependent lung ($P = 0.006$; fig. 4C). Such changes also showed differences at the regions of interest depending on the PEEP (ROI × PEEP: $P < 0.001$; fig. 4C). The intratidal changes in $V_{B_{tissue}}$ at PEEPs of 5 and 12 cm H_2O were similar with

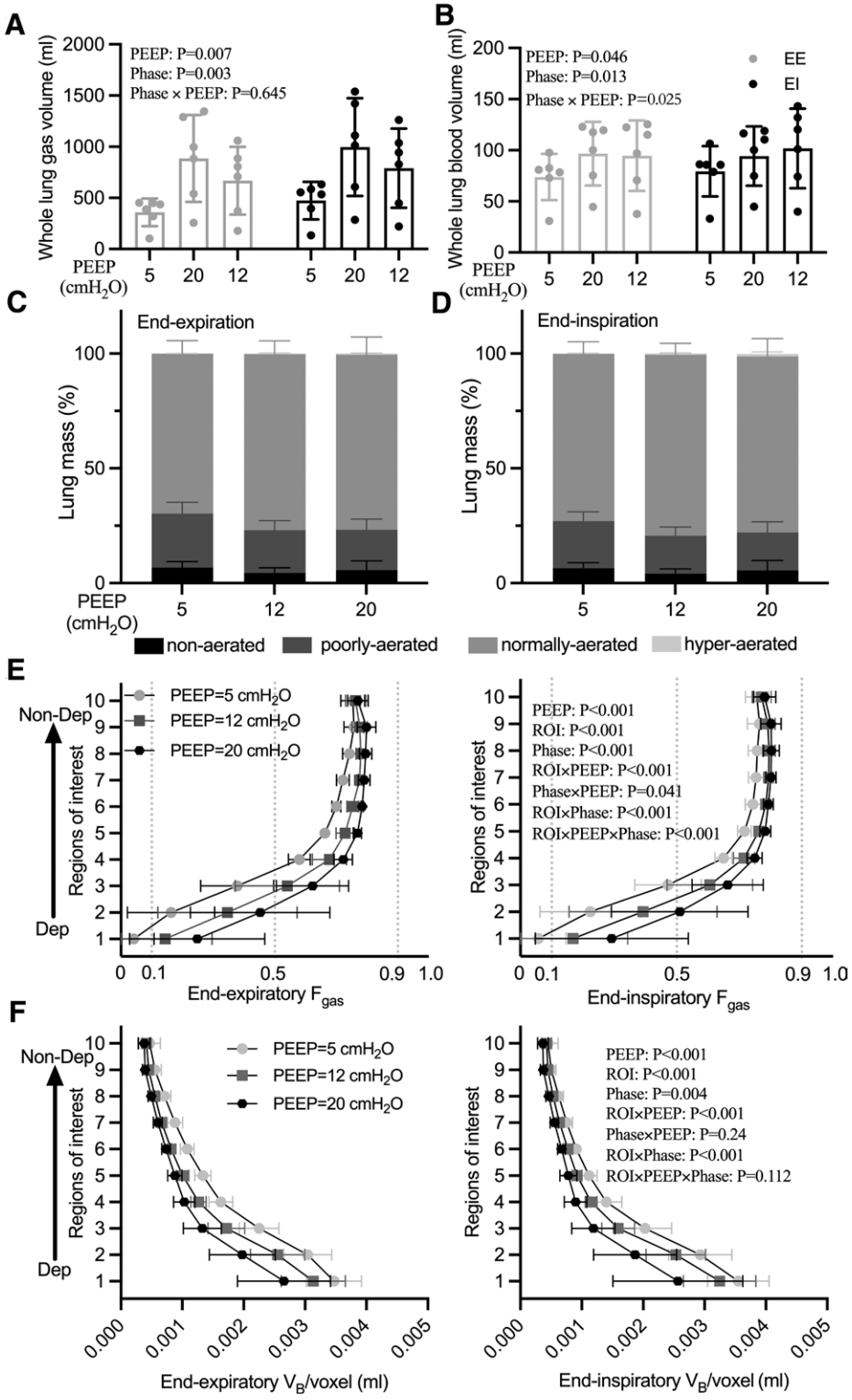

Fig. 2. (*A* and *B*) Whole-lung gas volume (*A*) and blood volume (*B*) at positive end-expiratory pressures (PEEPs) of 5, 12, and 20 cm H_2O in large animals with acute lung injury. (*C* and *D*) Lung mass with different aeration at end expiration (*C*) and end inspiration (*D*) at three PEEP levels. The values were calculated as percentages of whole-lung mass. Nonaerated, fraction of gas (F_{gas}) < 0.1; poorly aerated, 0.1 ≤ F_{gas} < 0.5; normally aerated, 0.5 ≤ F_{gas} < 0.9; and hyperaerated, F_{gas} ≥ 0.9. (*E*) Vertical distribution of mean lung aeration per voxel (F_{gas}) at end expiration (*left*) and end inspiration (*right*). (*F*) Vertical distribution of mean lung blood volume per voxel (V_B) at end expiration (*left*) and end inspiration (*right*). There were 10 regions of interest (ROIs) from dependent (Dep) to nondependent (Non-Dep) lungs.

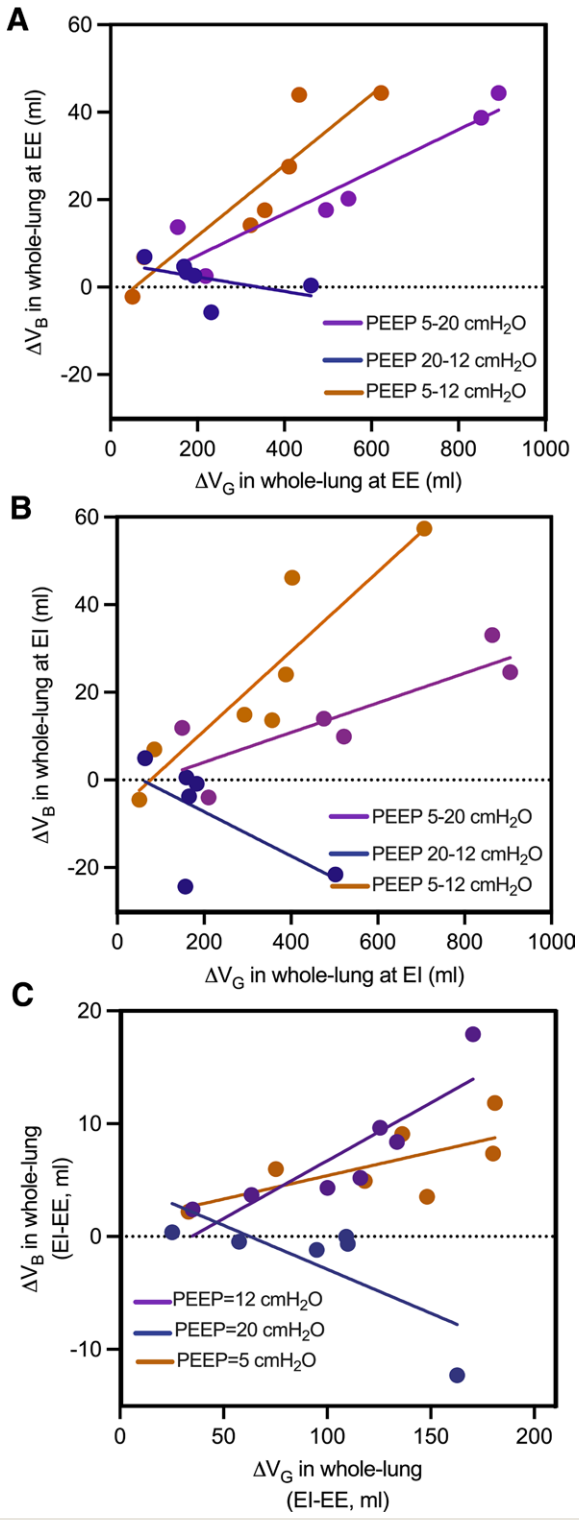

Fig. 3. (*A* and *B*) Whole-lung blood volume changes (ΔV_B) *versus* whole-lung gas volume changes (ΔV_G) at end expiration (EE; *A*) and end inspiration (EI; *B*). From positive end-expiratory pressures (PEEPs) of 5 to 20 cm H_2O, EE: slope = 0.047 (0.027, 0.068), $P < 0.001$; EI: slope = 0.034 (0.002, 0.065), $P = 0.037$; from PEEP = 20 to 12 cm H_2O, *(Continued)*

the gravitational patterns of tidal changes in F_{gas} (fig. 4D). In contrast, $V_{B_{tissue}}$ at a PEEP of 20 cm H_2O showed negative tidal changes in the middle regions despite *increased* F_{gas} in the same regions. Of note, a PEEP of 12 cm H_2O produced larger tidal changes of $V_{B_{tissue}}$ in all regions of interest except the middle regions.

Voxel-level $V_{B_{tissue}}$ presented a bimodal distribution in the nondependent, middle, and dependent lung at all PEEPs (fig. 4E). Such bimodality was predominantly observed at a PEEP of 5 cm H_2O, with a main peak at $V_{B_{tissue}} \approx 0.4$ and a secondary peak at $V_{B_{tissue}} \approx 0.1$, which was most evident in nondependent regions. In addition, lung regions of lowest $V_{B_{tissue}}$ ($V_{B_{tissue}} < 0.1$) were primarily found in the nondependent lung at all PEEP levels. Instead, relatively high $V_{B_{tissue}}$ ($V_{B_{tissue}} > 0.6$) were found with larger fractions predominantly in middle and dependent lungs.

Blood Volume Normalized to Gas Volume

To directly assess the amount of blood volume related to aerated volume, we computed voxel-wise V_B normalized to gas volume ($V_{B_{gas}}$). Similar to the distribution of $V_{B_{tissue}}$, $V_{B_{gas}}$ showed a gravitational dependence ($P = 0.002$; fig. 5A), with more than five times lower $V_{B_{gas}}$ in nondependent than dependent regions. As PEEP increased, $V_{B_{gas}}$ at each ROI decreased at both end expiration and end inspiration.

Different from regional distribution of $V_{B_{tissue}}$, regional $V_{B_{gas}}$ presented unimodal distributions in nondependent, middle, and dependent lungs at all PEEPs (fig. 5B). Lung regions with lower $V_{B_{gas}}$ were predominantly found in the nondependent lung, while relatively high $V_{B_{gas}}$ regions were mainly middle and dependent. PEEP increases resulted in a leftward shift (lower) $V_{B_{gas}}$ in all lung regions.

Discussion

Our main findings on the effects of different degrees of lung expansion produced with PEEP and dynamic tidal breathing on the distribution of pulmonary blood volume in a large animal model of endotoxemic and low-volume lung injury are that: (1) lung tissue–normalized blood volume presents a substantially heterogeneous spatial distribution, with large variation along the vertical axis, and is significantly influenced by lung expansion and the phase of mechanical ventilation (inspiration *vs.* expiration); (2)

Fig. 3. *(Continued)* EE: slope = –0.028 (–0.076, 0.019), P = 0.222; EI: slope = –0.050 (–0.120, 0.019), $P = 0.140$; and from PEEP = 5 to 12 cm H_2O, EE: slope = 0.084 (0.056, 0.112), $P < 0.001$; and EI: slope = 0.091 (0.048, 0.133), $P = 0.001$. (*C*) Intratidal whole-lung blood volume changes *versus* intratidal gas volume changes at each PEEP (5 cm H_2O: slope = 0.042 [–0.009, 0.092], $P = 0.101$; 20 cm H_2O: slope = –0.066 [–0.120, –0.011], $P = 0.021$; and 12 cm H_2O: slope = 0.086 [0.034, 0.139], $P = 0.003$).

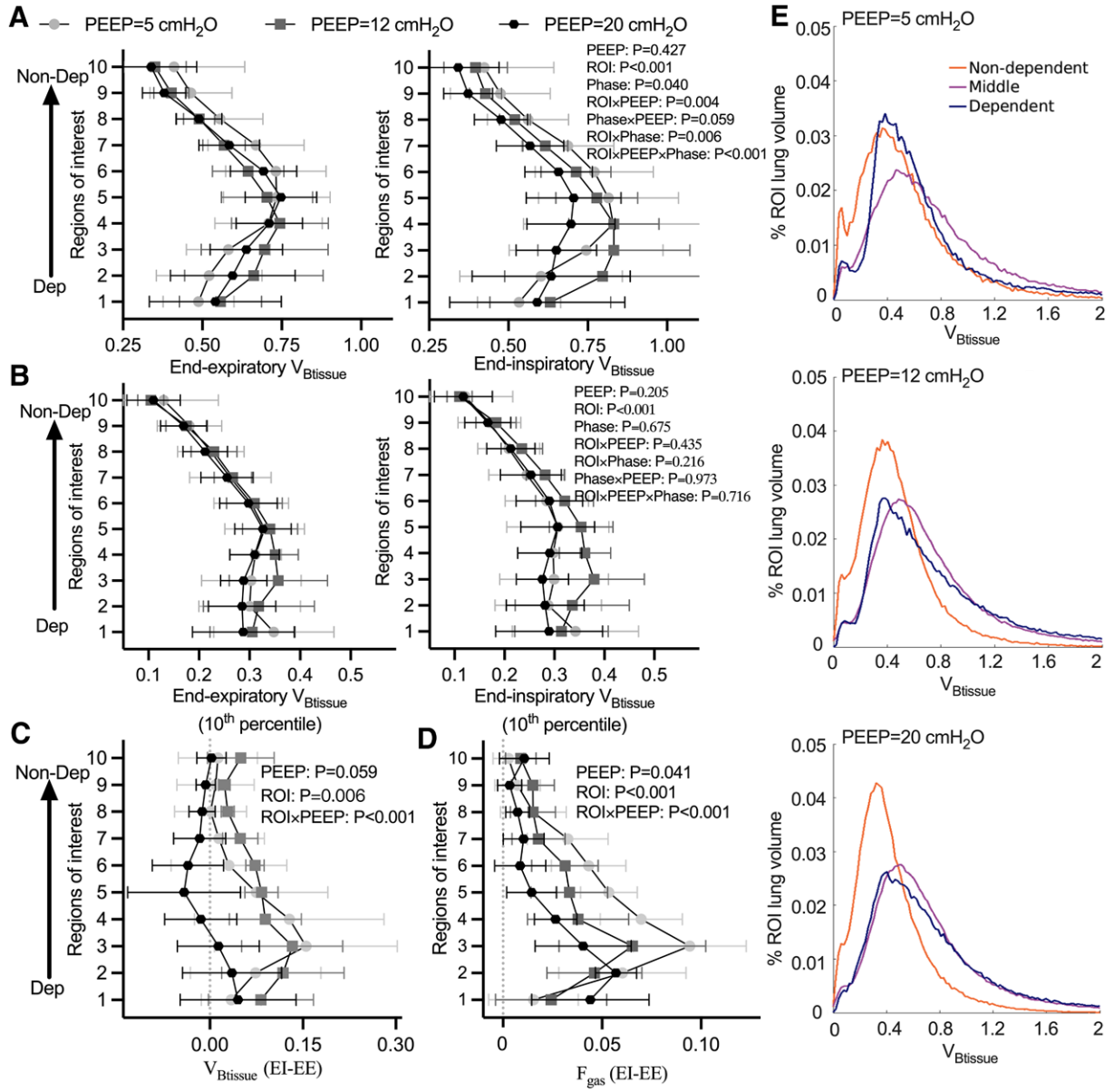

Fig. 4. (*A* and *B*) Vertical distribution of tissue-normalized blood volume ($V_{B_{tissue}}$; *A*) and its 10th percentile (*B*) with three positive end-expiratory pressures (PEEPs) at end expiration (EE) and end inspiration (EI). Ten regions of interest (ROIs) were presented from dependent (Dep) to nondependent (Non-Dep) lungs. (*C* and *D*) Intratidal changes of $V_{B_{tissue}}$ (*C*) and gas fraction (F_{gas}; *D*) along the vertical levels with three PEEP levels at end expiration and end inspiratory. (*E*) Regional distribution of $V_{B_{tissue}}$ in nondependent, middle, and dependent lungs with PEEPs or 5, 12, and 20 cm H_2O at end inspiration.

tissue-normalized blood volume in nondependent regions are substantially lower (approximately seven times lower) than means in mid-dependent regions with values close to zero indicating susceptibility to capillary closure; (3) an intermediate PEEP (12 cm H_2O) established from a recruited state and corresponding to the lowest transpulmonary pressure results in the most homogeneous distributions of tissue-normalized blood volume and the largest mean values in mid-dependent regions and inspiratory 10th percentile values throughout the lung, in contrast to both a lower (5 cm H_2O) and higher (20 cm H_2O) PEEP; and (4) whole-lung changes in blood volume positively correlate with corresponding changes of gas volume from PEEPs of 5 to 12 or 20 cm H_2O but not from PEEPs of 12 to 20 cm H_2O, suggesting small changes in vascular volume between recruited intermediate and high PEEP levels.

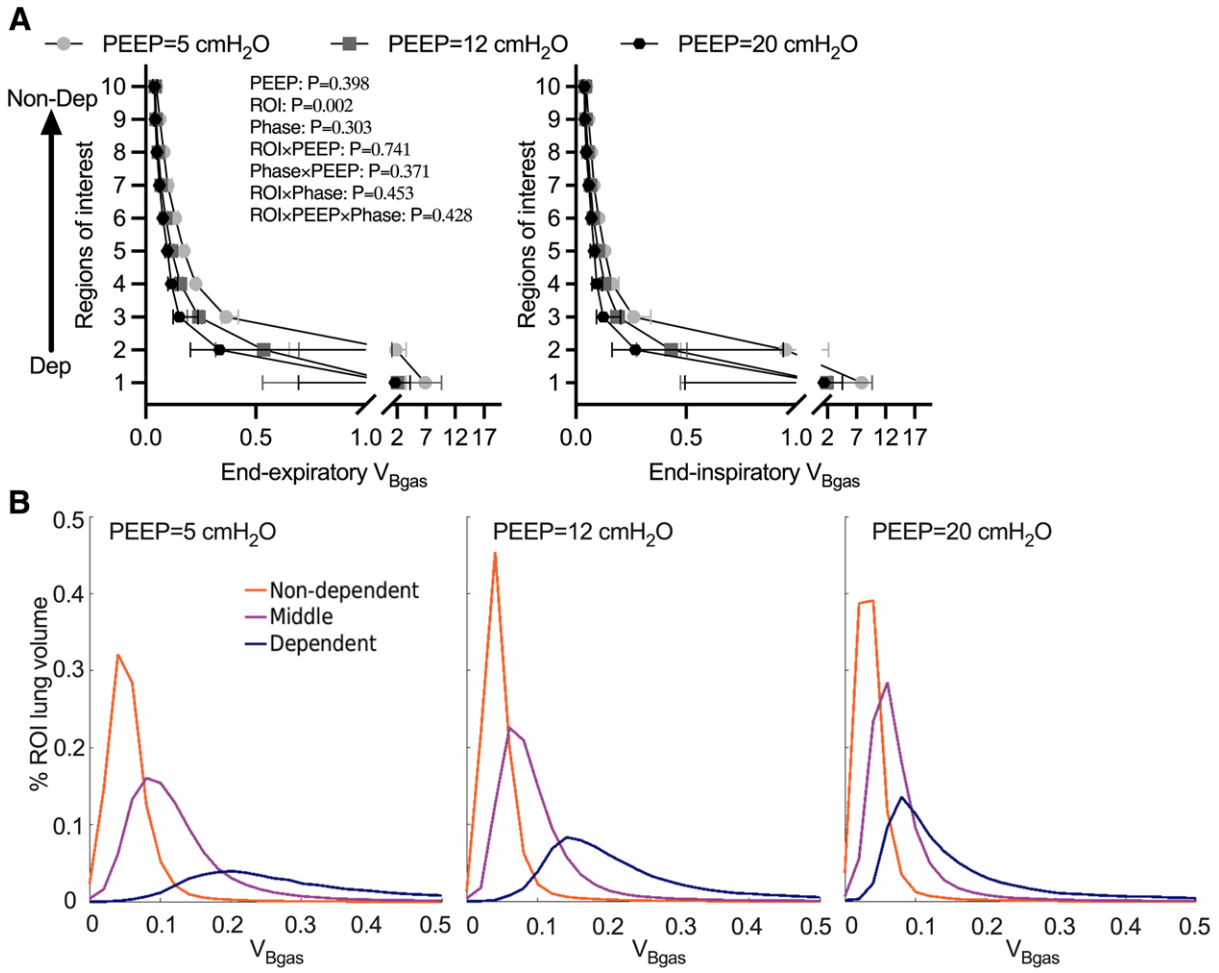

Fig. 5. (*A*) Vertical distribution of gas-normalized blood volume ($V_{B_{gas}}$) with positive end-expiratory pressures (PEEPs) of 5, 12, and 20 cm H_2O at end expiration and end inspiration. Ten regions of interest (ROIs) were presented from dependent (Dep) to nondependent (Non-Dep) lungs. (*B*) Regional distribution of $V_{B_{gas}}$ in nondependent, middle, and dependent lungs with PEEPs of 5, 12, and 20 cm H_2O at end inspiration.

Blood volume presented a clear gravitational ventral–dorsal gradient consistent with previous investigations in spontaneously breathing healthy humans[20] and findings of larger blood volume in collapsed regions of COVID-19 patients.[39] We computed tissue-normalized blood volume ($V_{B_{tissue}}$) to correct for the differences in lung inflation[40] and uniquely identify changes in the distribution of blood volume relative to tissue. If variations in regional blood volume were exclusively determined by the amount of tissue in different regions of interest, that ratio would be constant throughout the lungs. Instead, there was substantial heterogeneity of $V_{B_{tissue}}$ with similar coefficient of variation ~65% at end expiration and end inspiration. Of note, the coefficient of variation of $V_{B_{tissue}}$ was smallest at a PEEP of 12 cm H_2O. Such a PEEP value was chosen not only because it lies between the lower (5 cm H_2O) and higher (20 cm H_2O) tested PEEPs but also because it approximates the point of minimal respiratory and lung driving pressures and elastances in similar human and experimental conditions,[25–28] as it did in the current study, and provides beneficial local biomechanical effects.[23] Our results indicate that this point of lowest transpulmonary pressures established from a recruited higher PEEP level (20 cm H_2O) yielded the most homogeneous $V_{B_{tissue}}$ distribution, implying a vascular beneficial effect of that intermediate PEEP.

A systematic ventral–dorsal $V_{B_{tissue}}$ heterogeneity was observed, with lowest values in nondependent regions and the largest values in mid-dependent regions. There is minimal information on the spatial distribution of $V_{B_{tissue}}$. Our results are consistent with previous findings of gas diffusion inefficiency due to capillary blood volume changes beyond loss of aeration in mechanically ventilated anesthetized patients[6] and provide a spatial distribution basis for that inefficiency.

PEEP significantly affected the magnitude and spatial distribution of $V_{B_{tissue}}$. Of note, the effect of PEEP on

$V_{B_{tissue}}$ was not linearly associated with corresponding changes in gas volume expansion. While whole-lung gas volumes increased nearly linearly with PEEP in the broad studied range from 5 to 20 cm H_2O, whole-lung blood volume showed larger changes between PEEPs of 5 and 12 or 20 than between PEEPs of 20 and 12 cm H_2O. Thus, our results imply functional lung vascular recruitment or expansion between the low to intermediate or high PEEP levels but not between the intermediate and high PEEP levels. Given that a PEEP of 12 cm H_2O was achieved after a PEEP of 20 cm H_2O, this implies a preservation of vascular recruitment from 20 to 12 cm H_2O despite a reduction in lung aeration. Of note, tidal changes in $V_{B_{tissue}}$ at physiologic tidal volumes (8 ml/kg) showed that at PEEPs of 5 and 12 cm H_2O, inspiration produced small *increases* in $V_{B_{tissue}}$ in mid-dependent regions, while at a PEEP of 20 cm H_2O, inspiration-produced *reduction* of $V_{B_{tissue}}$ was observed. Such a reduction of $V_{B_{tissue}}$ at a PEEP of 20 cm H_2O, indicative of a maximum in ability of the pulmonary vasculature to recruit volume, could be due to the expansion effect of higher PEEP on extra-alveolar vessels counterbalanced by alveolar pressure compressing alveolar capillaries at the normal or mildly increased vascular pressures present in this clinically relevant model. Additionally, heart–lung interactions could contribute to the effect of lung expansion from PEEP on whole-lung and regional lung blood volume, because high PEEP reduces systemic venous return *via* decreasing cardiac output and increasing right ventricular afterload. Considering that larger V_C results in larger diffusing capacity[2] and potentially lower risk for injury,[4,5] overall, our results imply that an intermediate PEEP established from a recruited state brings functional and lung-protective vascular expansion benefits beyond the lung aeration and strain benefits previously reported.[25,41] Our results also expand previous findings of a *negative* relationship between gas and blood volume changes with PEEP and tidal volume in normal lungs,[9] when neither substantial alveolar or capillary collapse are expected to be present, in contrast to our findings in lung injury.

Regionally, mean $V_{B_{tissue}}$ at a PEEP of 12 cm H_2O in mid-dependent regions was larger than that at a PEEP of 5 or 20 cm H_2O. A PEEP of 12 cm H_2O also produced a consistently larger 10th percentile of $V_{B_{tissue}}$ at end inspiration, *i.e.*, higher minimal values of $V_{B_{tissue}}$, suggesting lower risk for capillary collapse during the breathing cycle. Additionally, a PEEP of 12 cm H_2O promoted blood to redistribute to nondependent (*i.e.*, highly aerated) regions during inhalation, consistent with reduced susceptibility to lung injury[3] and reduced alveolar dead space[42] and contrasting with observations in normal lungs[9] and during a PEEP of 5 or 20 cm H_2O. Such results reinforce the regional functional and potentially protective advantages of an intermediate PEEP.

$V_{B_{tissue}}$ distributions revealed very low values in nondependent lung regions in all conditions, with a PEEP of 5 cm H_2O showing the clearest secondary peaks at $V_{B_{tissue}} \approx 0.1$. The presence of very low $V_{B_{tissue}}$ can also be noted in the nondependent 10th percentile $V_{B_{tissue}}$ approximately seven times lower than the mean values in the normally aerated middle regions. These findings are consistent with histologic evidence of collapsed alveolar capillaries and open extra-alveolar capillaries (corner vessels) at high levels of lung expansion.[11,12] They also match previous reports of absent blood flow in nondependent regions of large animals at usual airway pressures[5] and hyperinflated regions in rats.[4] The high-normal nondependent aeration ($F_{gas} > 0.7$) together with the similar 10th percentile of $V_{B_{tissue}}$ for the studied PEEPs suggest that a condition of maximal expansion could have been reached in these regions, with the very low nonzero $V_{B_{tissue}}$ representing predominantly extra-alveolar capillaries. Given that cyclic capillary collapse can produce lung injury during exaggerated tidal volume ventilation,[3,4] our results imply that regional conditions for such injurious mechanism could occur within the range of mechanical ventilator settings used clinically.

This study has limitations. We utilized a large animal model assessed during pressure-controlled ventilation and systemic inflammation (*i.e.*, mild-moderate systemic endotoxemia + atelectasis) receiving total intravenous general anesthesia. Accordingly, our results cannot be directly extrapolated to severe ARDS, other ventilation modes, or volatile anesthetics, which have distinct effects on the pulmonary circulation.[43–45] The use of a fixed sequence of PEEP values could have produced carryover effects in our findings. This sequence aimed to produce a clear distinction in lung expansion and blood volume distributions between a well-established initial derecruited state at a PEEP of 5 cm H_2O and a highly recruited state at a PEEP of 20 cm H_2O.[23,25] It also provided those distributions at an intermediate PEEP (12 cm H_2O) found to provide biomechanical benefits[23] and to relate to low transpulmonary pressures, as observed in the current article. Such a sequence could have contributed to the similarities between PEEPs of 20 and 12 cm H_2O. Imaging was performed after stabilization of respiratory mechanics, ~27 min between changes in PEEP, presumably minimizing carryover effects. We focused on pulmonary blood volume distribution at different levels of lung expansion produced by PEEPs within clinical ranges in injured lungs and did not explore their difference from baseline.

In summary, we demonstrate that there is substantial variability in the distribution of lung blood volume beyond that related to lung expansion during acute lung injury in large animals with lung size and function comparable to those of humans. Ventilator settings within the clinical range can be associated with

susceptibility to capillary collapse particularly in non-dependent regions. An intermediate PEEP level (12 cm H_2O) established from a recruited state and presenting respiratory system and transpulmonary driving pressures lower than those at PEEPs of 5 or 20 cm H_2O yielded the most homogeneous distributions of tissue-normalized blood volume, with the largest values of mean in mid-dependent regions and the largest 10th percentile throughout the lung consistent with a vascular protective effect. Changes in pulmonary blood volume with gas volume recruited by PEEP indicate a maximum of vascular volume recruitment at that intermediate PEEP.

Acknowledgments

The authors thank Steve Weise, B.S., and John A. Correia, Ph.D. (Department of Radiology, Nuclear Medicine and Molecular Imaging, and Cyclotron Unit, Massachusetts General Hospital, Boston, Massachusetts), for the expert technical support with computed tomographic and positron emission tomographic imaging.

Research Support

Supported by National Institutes of Health/National Heart, Lung, and Blood Institute (Bethesda, Maryland) grant No. R01 HL121228. Supported in part by funds from Fundação de Amparo à Pesquisa do Estado do Rio de Janeiro (Rio de Janeiro, Brazil; to Dr. Motta-Ribeiro).

Competing Interests

The authors declare no competing interests.

Correspondence

Address correspondence to Dr. Zeng: 650 West 168th Street, BB724, New York, New York 10032. cz2703@cumc.columbia.edu

Supplemental Digital Content

Supplemental Methods, https://links.lww.com/ALN/D889

References

1. Burchardi H, Stokke T: Pulmonary diffusing capacity for carbon monoxide by rebreathing in mechanically ventilated patients. Bull Eur Physiopathol Respir 1985; 21:263–73
2. Roughton FJ, Forster RE: Relative importance of diffusion and chemical reaction rates in determining rate of exchange of gases in the human lung, with special reference to true diffusing capacity of pulmonary membrane and volume of blood in the lung capillaries. J Appl Physiol 1957; 11:290–302
3. Katira BH, Kuebler WM, Kavanagh BP: Inspiratory preload obliteration may injure lungs via cyclical "on–off" vascular flow. Intensive Care Med 2018; 44:1521–3
4. Katira BH, Giesinger RE, Engelberts D, et al.: Adverse heart–lung interactions in ventilator-induced lung injury. Am J Respir Crit Care Med 2017; 196:1411–21
5. Motta-Ribeiro GC, Winkler T, Costa ELV, de Prost N, Tucci MR, Vidal Melo MF: Worsening of lung perfusion to tissue density distributions during early acute lung injury. J Appl Physiol (1985) 2023; 135:239–50
6. Di Marco F, Bonacina D, Vassena E, et al.: The effects of anesthesia, muscle paralysis, and ventilation on the lung evaluated by lung diffusion for carbon monoxide and pulmonary surfactant protein B. Anesth Analg 2015; 120:373–80
7. Macnaughton PD, Morgan CJ, Denison DM, Evans TW: Measurement of carbon monoxide transfer and lung volume in ventilated subjects. Eur Respir J 1993; 6:231–6
8. Di Marco F, Devaquet J, Lyazidi A, et al.: Positive end-expiratory pressure-induced functional recruitment in patients with acute respiratory distress syndrome. Crit Care Med 2010; 38:127–32
9. Porra L, Broche L, Dégrugilliers L, et al.: Synchrotron imaging shows effect of ventilator settings on intra-breath cyclic changes in pulmonary blood volume. Am J Respir Cell Mol Biol 2017; 57:459–67
10. West JB, Dollery CT, Naimark A: Distribution of blood flow in isolated lung: Relation to vascular and alveolar pressures. J Appl Physiol 1964; 19:713–24
11. Hedenstierna G, White FC, Mazzone R, Wagner PD: Redistribution of pulmonary blood flow in the dog with PEEP ventilation. J Appl Physiol Respir Environ Exerc Physiol 1979; 46:278–87
12. Nieman GF, Paskanik AM, Bredenberg CE: Effect of positive end-expiratory pressure on alveolar capillary perfusion. J Thorac Cardiovasc Surg 1988; 95:712–6
13. Brudin LH, Rhodes CG, Valind SO, Wollmer P, Hughes JM: Regional lung density and blood volume in non-smoking and smoking subjects measured by PET. J Appl Physiol (1985) 1987; 63:1324–34
14. Musch G, Layfield JDH, Harris RS, et al.: Topographical distribution of pulmonary perfusion and ventilation, assessed by PET in supine and prone humans. J Appl Physiol (1985) 2002; 93:1841–51
15. Santos A, Motta-Ribeiro GC, De Prost N, et al.: Regional pulmonary perfusion, blood volume, and their relationship change in experimental early ARDS. Sci Rep 2024; 14:5832
16. Wellman TJ, Winkler T, Vidal Melo MF: Modeling of tracer transport delays for improved quantification of regional pulmonary ^{18}F-FDG kinetics, vascular transit times, and perfusion. Ann Biomed Eng 2015; 43:2722–34

17. Prost N de, Feng Y, Wellman T, et al.: ^{18}F-FDG kinetics parameters depend on the mechanism of injury in early experimental acute respiratory distress syndrome. J Nucl Med 2014; 55:1871–7
18. Cronin JN, Crockett DC, Farmery AD, et al.: Mechanical ventilation redistributes blood to poorly ventilated areas in experimental lung injury. Crit Care Med 2020; 48:e200–8
19. Brudin LH, Rhodes CG, Valind SO, Jones T, Hughes JM: Interrelationships between regional blood flow, blood volume, and ventilation in supine humans. J Appl Physiol (1985) 1994; 76:1205–10
20. Brudin LH, Rhodes CG, Valind SO, Jones T, Jonson B, Hughes JM: Relationships between regional ventilation and vascular and extravascular volume in supine humans. J Appl Physiol (1985) 1994; 76:1195–204
21. National Research Council Committee for the Update of the Guide for the Care and Use of Laboratory Animals: Guide for the Care and Use of Laboratory Animals, 8th edition. Washington, D.C., National Academies Press, 2011
22. Percie du Sert N, Hurst V, Ahluwalia A, et al.: The ARRIVE guidelines 2.0: Updated guidelines for reporting animal research. PLoS Biol 2020; 18:e3000410
23. Lagier D, Zeng C, Kaczka DW, et al.: Mechanical ventilation guided by driving pressure optimizes local pulmonary biomechanics in an ovine model. Sci Transl Med 2024; 16:eado1097
24. Karbing DS, Panigada M, Bottino N, et al.: Changes in shunt, ventilation/perfusion mismatch, and lung aeration with PEEP in patients with ARDS: A prospective single-arm interventional study. Crit Care 2020; 24:111
25. Zeng C, Zhu M, Motta-Ribeiro G, et al.: Dynamic lung aeration and strain with positive end-expiratory pressure individualized to maximal compliance versus ARDSNet low-stretch strategy: A study in a surfactant depletion model of lung injury. Crit Care 2023; 27:307
26. Pintado M-C, de Pablo R, Trascasa M, et al.: Individualized PEEP setting in subjects with ARDS: A randomized controlled pilot study. Respir Care 2013; 58:1416–23
27. Fernandez-Bustamante A, Sprung J, Parker RA, et al.: Individualized PEEP to optimise respiratory mechanics during abdominal surgery: A pilot randomised controlled trial. Br J Anaesth 2020; 125:383–92
28. Ferrando C, Soro M, Unzueta C, et al.; Individualized PeRioperative Open-lung VEntilation (iPROVE) Network: Individualised perioperative open-lung approach versus standard protective ventilation in abdominal surgery (iPROVE): A randomised controlled trial. Lancet Respir Med 2018; 6:193–203
29. Shi C, Tang X, Chan M: Evaluation of the new respiratory gating system. Precis Radiat Oncol 2017; 1:127–33
30. Motta-Ribeiro GC, Hashimoto S, Winkler T, et al.: Deterioration of regional lung strain and inflammation during early lung injury. Am J Respir Crit Care Med 2018; 198:891–902
31. Reumuth G, Alharbi Z, Houschyar KS, et al.: Carbon monoxide intoxication: What we know. Burns 2019; 45:526–30
32. Shi C, Tang X, Chan M: Evaluation of the new respiratory gating system. Precis Radiat Oncol 2017; 1:127–33
33. Gerard SE, Herrmann J, Kaczka DW, Musch G, Fernandez-Bustamante A, Reinhardt JM: Multi-resolution convolutional neural networks for fully automated segmentation of acutely injured lungs in multiple species. Med Image Anal 2020; 60:101592
34. Chang G, Chang T, Pan T, Clark JW, Mawlawi OR: Joint correction of respiratory motion artifact and partial volume effect in lung/thoracic PET/CT imaging. Med Phys 2010; 37:6221–32
35. Bogot NR, Steiner R, Helviz Y, et al.: Distribution of aeration and pulmonary blood volume in healthy, ARDS and COVID-19 lungs: A dual-energy computed tomography retrospective cohort study. Acad Radiol 2023; 30:2548–56
36. Hurtado DE, Erranz B, Lillo F, et al.: Progression of regional lung strain and heterogeneity in lung injury: Assessing the evolution under spontaneous breathing and mechanical ventilation. Ann Intensive Care 2020; 10:107
37. Prost N de, Costa EL, Wellman T, et al.: Effects of ventilation strategy on distribution of lung inflammatory cell activity. Crit Care 2013; 17:R175
38. R Core Team: R: A language and environment for statistical computing. Vienna, Austria, R Foundation for Statistical Computing, 2023
39. Ball L, Robba C, Herrmann J, et al.: Lung distribution of gas and blood volume in critically ill COVID-19 patients: A quantitative dual-energy computed tomography study. Crit Care 2021; 25:214
40. de Prost N, Costa EL, Wellman T, et al.: Effects of surfactant depletion on regional pulmonary metabolic activity during mechanical ventilation. J Appl Physiol (1985) 2011; 111:1249–58
41. Pereira SM, Tucci MR, Morais CCA, et al.: Individual positive end-expiratory pressure settings optimize intraoperative mechanical ventilation and reduce postoperative atelectasis. Anesthesiology 2018; 129:1070–81
42. Beda A, Winkler T, Wellman TJ, De Prost N, Tucci M, Vidal Melo MF: Physiological mechanism and spatial distribution of increased alveolar dead-space in early ARDS: An experimental study. Acta Anaesthesiol Scand 2021; 65:100–8
43. Pagel PS, Fu JL, Damask MC, et al.: Desflurane and isoflurane produce similar alterations in systemic and pulmonary hemodynamics and arterial oxygenation in

patients undergoing one-lung ventilation during thoracotomy. Anesth Analg 1998; 87:800–7
44. Kerbaul F, Bellezza M, Guidon C, et al.: Effects of sevoflurane on hypoxic pulmonary vasoconstriction in anaesthetized piglets. Br J Anaesth 2000; 85:440–5
45. Benumof JL, Augustine SD, Gibbons JA: Halothane and isoflurane only slightly impair arterial oxygenation during one-lung ventilation in patients undergoing thoracotomy. Anesthesiology 1987; 67:910–5